

# Electrosynthesis of high-entropy sulfides/graphene composites for advanced energy storage

PI: Zhenyuan Xia

## 1. Project overview

The aim of this project was to explore an electrochemical route for the synthesis of multi-component sulfide materials integrated with graphene, with the long-term perspective of developing high-entropy sulfide systems for advanced energy storage. The goal was to establish a direct and scalable electrochemical process to replace conventional high-temperature, multi-step synthesis routes, while enhancing conductivity, structural stability, and electrochemical activity via graphene integration.

## 2. Results and discussion

The main result of the project is the establishment of a direct electrochemical deposition strategy that allows the construction of high-entropy transition metal sulfides on conductive substrates. In practice, Ni, Co, Mn, Fe and Cr sulfide systems were synthesized in a single step, directly on three-dimensional graphene-based frameworks. This approach avoids the complexity of traditional synthesis routes and provides a high degree of control over both composition and morphology under mild conditions.

The electrochemical performance of our high-entropy sulfide catalyst surpasses that of commercial PtRuC benchmarks across all critical metrics. Specifically, the synergistic effect between the multi-metal composition and the graphene framework facilitates rapid kinetics for water oxidation and oxygen reduction, resulting in Zn–air batteries with an impressive energy density of 1001 Wh kg<sup>-1</sup>.

The synthesis of multi-metal sulfides and graphene layers were done by separate electrophoretic deposition and cyclic voltammetry deposition method under room temperature with mild aqueous conditions. We have successfully fabricated NiCoMnS<sub>x</sub> (NCMS), NiCoMnFeS<sub>x</sub> (NCMFS), and NiCoMnFeCrS<sub>x</sub> (NCMFCS) with graphene interface through our electrochemical strategy.

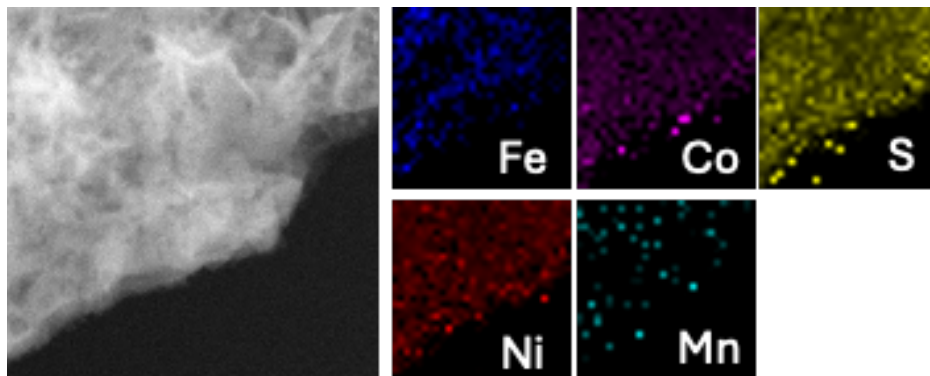


**Figure 1.** STEM-HAADF micrograph of the NCMFS with the corresponding Ni, Co Mn, and Fe elements from STEM-EDS mapping.

The detailed morphology and composition of the structure was studied by scanning electron microscopy (SEM) and transmission electron microscopy (TEM). For example, Figure 1 clearly shows the selected area electron diffraction (SAED) results from NCMFS, with a homogenous distribution of metal cations and sulfur on the graphene substrate, demonstrating the co-existence of Ni, Co, Mn, Fe and S elements.

To understand the initial electronic status of our samples, we also performed the ex-situ Near Edge X-ray Absorption Fine Structure (NEXAFS) spectroscopy. Both quaternary and quinary metal sulfides show clear  $L_3$  and  $L_2$  edges for the corresponding transition metals from both fluorescence yield (FY) and total electron yield (TEY) modes.

As shown in Figure 2, the four metal NCMFS sample, including Ni, Co, Fe and Mn were clearly identified by their characteristic TEY and FY peaks. The main peak at 854 eV, with a shoulder at 855.7 eV in the TEY spectrum at the  $L_3$ -edge, indicates the oxidation state of  $Ni^{2+}$  in the mixed metal sulfides. A similar shape is observed in the FY spectrum, but with a relatively higher shoulder peak. Figure 1b reveals the oxidation state of  $Co^{2+}$ , as indicated by its typical multiple XAS peaks (centered at 779.7 eV) at the  $L_3$ -edge in the TEY data. The FY spectrum for the Co  $L$ -edge also shows a similar pattern to the TEY spectrum. Figure 1c indicates the mixed oxidation states of  $Fe^{2+}$  and  $Fe^{3+}$ , based on the two TEY peaks at 709.6 eV and 711.5 eV. Figure 1d shows the oxidation states of both  $Mn^{3+}$  and  $Mn^{4+}$ , with corresponding peaks at 641.9 eV and 643.2 eV. Similar TEY and FY results also suggest that the oxidation status of these 3d transition metals are consistent both on the surface and in the bulk.

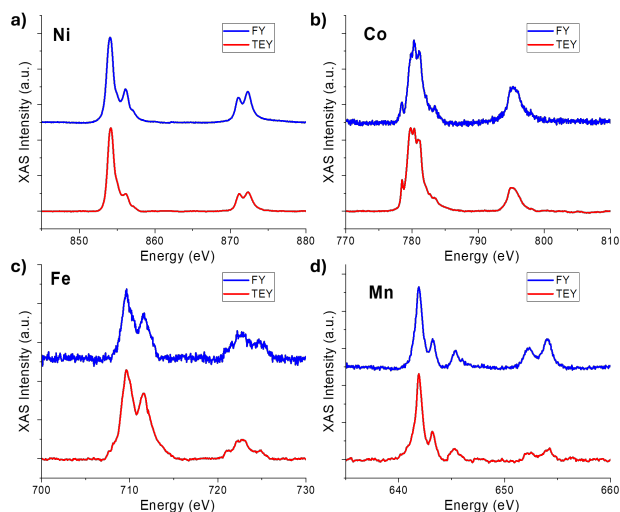


**Figure 2.** The  $L_{2,3}$ -edge XAS spectra for transition metals from NCMFS sample taken by TEY FY detection modes, a) the Ni  $L_{2,3}$ -edge NEXAFS spectra, b) Co  $L_{2,3}$ -edge NEXAFS spectra, c) Fe  $L_{2,3}$ -edge NEXAFS spectra, d) Mn  $L_{2,3}$ -edge NEXAFS spectra.

Similar to the quaternary metal sulfides, the quinary metal sulfide containing Ni, Co, Fe, Mn, and Cr demonstrate nearly identical TEY and FY XAS spectra for the NCMFCS

sample, as shown in Figures 3. For the Cr L<sub>2,3</sub>-edge TEY and FY results, two peaks at 578.2 eV and 579.2 eV suggest the presence of mixed valence states, Cr<sup>3+</sup> and Cr<sup>4+</sup>, in the metal sulfides.

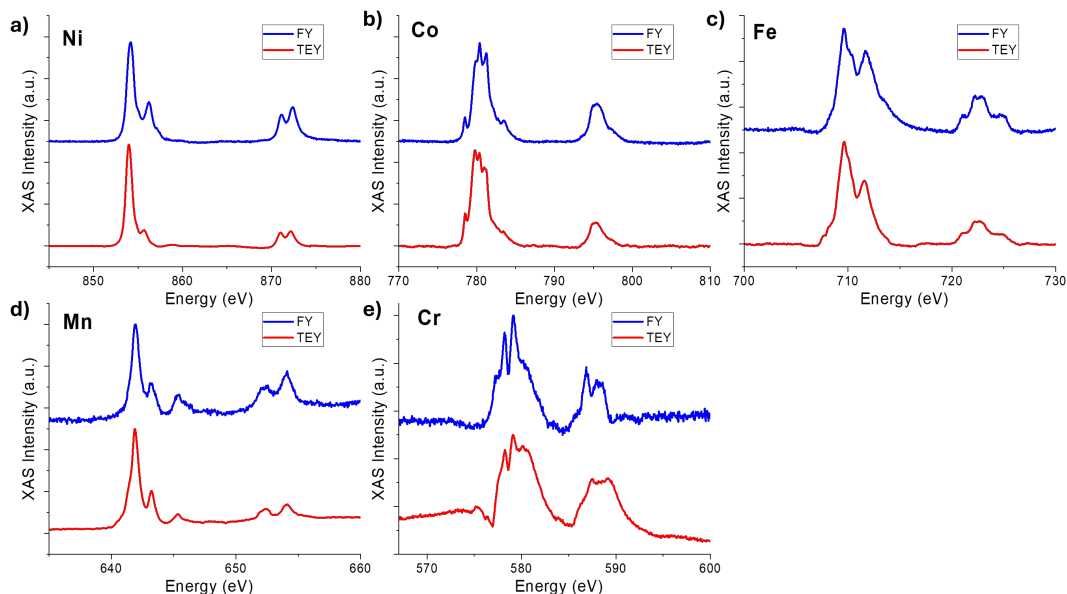


**Figure 3.** The L<sub>2,3</sub>-edge XAS spectra for transition metals from NCMFCS sample taken by TEY FY detection modes, a) the Ni L<sub>2,3</sub>-edge NEXAFS spectra, b) Co L<sub>2,3</sub>-edge NEXAFS spectra, c) Fe L<sub>2,3</sub>-edge NEXAFS spectra, d) Mn L<sub>2,3</sub>-edge NEXAFS spectra, e) Cr L<sub>2,3</sub>-edge NEXAFS spectra.

Following the element and morphology characterization, the electrocatalytic performance of our materials for oxygen evolution and reduction reactions were tested by rotating disk/ring-disk electrodes (RDE/RRDE). Nitrogen-doped reduced graphene oxide (NrGO) was used as the interface for mixed metal sulfides, and graphene foam was used as the matrix for the loading of both NrGO and sulfides. The results were shown in Figure 4. In the anodic region, the linear sweep voltammetry (LSV) curves (Figure 4b) demonstrate that both FeCoMnNiS/NrGO/GF (NCMFS) and the chromium added FeCoMnNiCrS/NrGO/GF (NCMFCS) electrode exhibits superior OER kinetics, achieving a benchmark current density of 10 mA cm<sup>-2</sup> at a low potential of 1.53 V and 1.55 V vs. RHE, respectively. The prominent redox peaks observed between 1.3 V and 1.5 V suggest the surface reconstruction of metal sulfides into oxyhydroxide active phases, which are traditionally responsible for facilitating the four-electron water oxidation process. Complementary to the anodic performance, the cathodic ORR profiles (Figure 4c) highlight the bifunctional nature of the catalysts. The NCMFS electrode displays a more positive onset potential and a higher diffusion-limiting current density compared to the NCMFCS sample, reaching nearly -10 mA cm<sup>-2</sup>. The characteristic plateau-like regions in the ORR curves suggest a multi-step reduction mechanism, likely dominated by the efficient four-electron pathway ( $O_2 + 2H_2O + 4e^- \rightarrow 4OH^-$ ). Collectively, the reduced overpotentials and high current densities confirm that the multi-metal sulfide architecture on a conductive graphene-functionalized scaffold provides a synergistic environment for reversible oxygen

electrochemistry, making it a promising candidate for integrated energy storage and conversion devices.

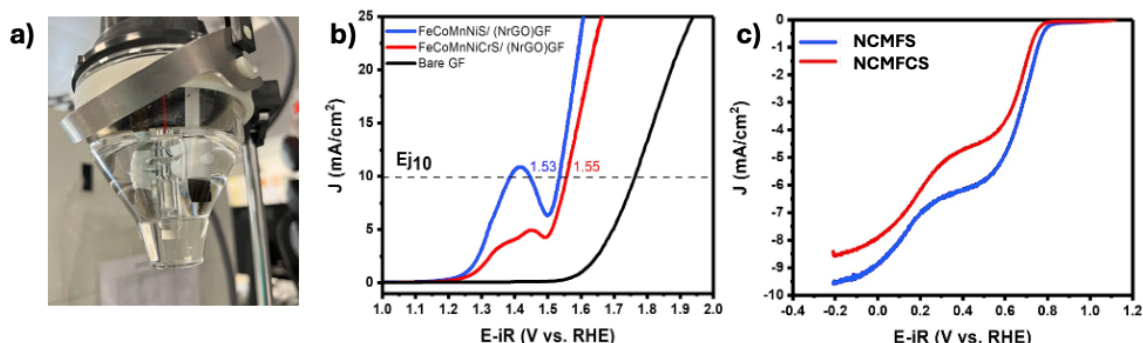


**Figure 4.** a) 3-electrode set up for the electrochemical analysis of the electrodes b) OER curves recorded for the electrodes in N<sub>2</sub> saturated 0.1M KOH c) ORR curves for the electrodes in O<sub>2</sub> saturated 0.1M KOH.

We also evaluated the performance of our multi-metal sulfide/graphene composites in energy storage devices. The NCMS/NrGO-GF catalyst demonstrates exceptional performance as a bifunctional air cathode in rechargeable Zn–air batteries (ZABs), as illustrated in the 3D-printed cell assembly (Figure 5a). It achieves a stable open-circuit voltage of 1.42 V (Figure 5b) and a high specific capacity of 815.5 mAh g<sub>Zn</sub><sup>-1</sup> when discharged at 10 mA cm<sup>-2</sup> (Figure 5c), outperforming the commercial PtRuC benchmark.

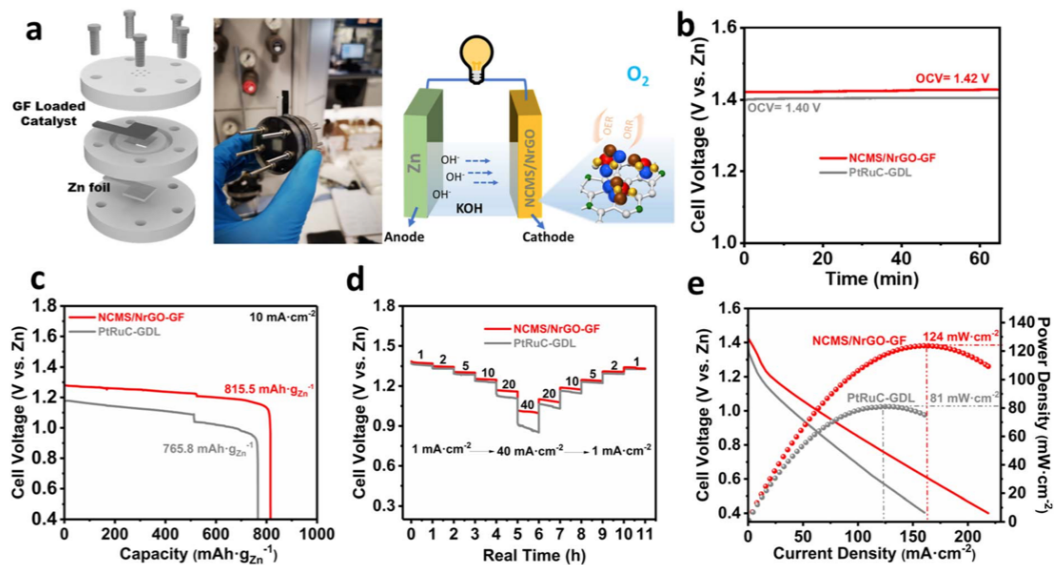


**Figure 5.** a) Schematic illustration of a 3D-printed Zn–air cell. b) Open circuit voltage of NCMS/NrGO-GF cells and PtRuC cells. c) Discharge curve of Zn–air batteries with NCMS/NrGO and PtRuC as oxygen electrode catalysts at 10 mA cm<sup>-2</sup>. d) Discharge profiles of the Zn–air battery based on NCMS/NrGO-GF and PtRuC-GDL catalyst electrodes at various current densities. e) Galvanodynamic discharge profile and power density curve of NCMS/NrGO-GF and PtRuC-GDL air cathodes.

## Final Report – ÅForsk Project No. 222-263

This leads to an impressive energy density of  $1001 \text{ W h kg}_{\text{Zn}}^{-1}$ , which is ca. 92% of the theoretical maximum, signaling the material's high efficiency in converting chemical energy into electrical power.

Further evaluation indicates superior rate capability and power output compared to noble-metal catalysts. The NCMS/NrGO-GF battery maintains stable discharge plateaus across a wide range of current densities, from 1 to  $40 \text{ mA cm}^{-2}$  (Figure 5d), and delivers a peak power density of  $124 \text{ mW/cm}^2$  (Figure 5e). These results, combined with the material's stable round-trip voltage and long-term cycling stability, confirm that the integration of entropy stabilized multi-metal sulfides onto a 3D graphene foam scaffold provides a robust, highly active interface for reversible oxygen electrochemistry in practical energy storage applications.

### 3. Conclusions

This project demonstrates that electrochemical synthesis can be used to directly construct multi-metal sulfide/graphene composites with well-defined hierarchical structures and strong electrochemical performance. The developed materials show high activity and durability, which can be traced back to the interplay between multi-metal composition, nanoscale architecture, and conductive graphene frameworks.

More importantly, the work provides a clear pathway toward the realization of high-entropy sulfide systems. By showing that multiple metal species can be incorporated and controlled within a single electrochemical process, the project establishes a scalable foundation for future developments of electrochemical synthesis in the fabrication of advanced materials.

As a result, the support from the Åforsk Foundation (Project No. 222-263) has been instrumental in the publication of four peer-reviewed papers, with the focus on the development and application of advanced electrochemical methods for graphene-based materials and composites:

[1] Zhang, X.; Xia, Z.; et al. Producing bilayer graphene oxide via wedge ion-assisted anodic exfoliation. *ACS Applied Nano Materials* 2023, 6, 20049–20058. <https://doi.org/10.1021/acsanm.3c03047>

[2] Xia, Z.; Asp, L. E.; et al. Graphene additives for structural battery composites with improved multifunctional performance. *Composites Science and Technology* 2024, 243, 110195. <https://doi.org/10.1016/j.compscitech.2024.110195>

[3] Kovtun, A.; Xia, Z.; et al. Graphene-based composite materials for advanced electrochemical energy applications. *Journal of Materials Chemistry A* 2024, 12, 12345–12358. <https://doi.org/10.1039/D3TA07765A>

[4] Xia, Z.; et al. Electrochemical 3D printing of copper/graphene composite architectures. *Additive Manufacturing* 2025, 76, 103650. <https://doi.org/10.1016/j.addma.2025.103650>